

## Ultrathin Aluminum Oxide Tunnel Barriers

W. H. Rippard, A. C. Perrella, F. J. Albert, and R. A. Buhrman

*School of Applied and Engineering Physics, Cornell University, Ithaca, New York 14853-2501*

(Received 20 June 2001; published 15 January 2002)

Ballistic electron emission microscopy is used to study the formation of ultrathin tunnel barriers by the oxidation of aluminum. An O<sub>2</sub> exposure, ~30 mTorr sec, forms a uniform tunnel barrier with a barrier height  $\phi_b$  of 1.2 eV. Greater O<sub>2</sub> exposure does not alter  $\phi_b$  or the ballistic transmissivity of the oxide conduction band. Tunneling spectroscopy indicates a broad energy distribution of electronic states in the oxide. With increasing O<sub>2</sub> dose the states below 1.2 eV gradually become localized, but until this localization is complete these states can provide low-energy single-electron channels through the oxide.

DOI: 10.1103/PhysRevLett.88.046805

PACS numbers: 73.40.Gk, 68.37.-d

Very thin aluminum oxide (AlO<sub>x</sub>) layers, formed either by ~20 °C thermal oxidation or by plasma oxidation of Al layers, have long been employed as the barrier layer in tunnel junctions. Earlier, a Nb-AlO<sub>x</sub>-Al-Nb thin film process was developed for the fabrication of high-quality Josephson junctions (JJs) [1]. More recently, magnetic tunnel junctions (MTJs) consisting of ferromagnetic electrodes and an AlO<sub>x</sub> barrier layer have exhibited high tunneling magnetoresistances [2]. Much junction research is focused on ultrathin, highly transparent barriers, which are required for tunneling devices if they are to exhibit the impedance level (for MTJs) [3] and critical current density  $J_c$  (for JJs) [4] necessary for nanoscale research and future applications. A MTJ with specific resistance  $\leq 1 \Omega \mu\text{m}^2$  will eventually be required for hard disk read head applications, while  $J_c \geq 2 \times 10^5 \text{ A/cm}^2$  is needed for very high-speed nanoscale JJ devices. This necessitates a tunnel barrier with an overall transparency  $\geq 10^{-3}$ , which raises the basic question—how thin and transparent can a given insulating layer be and still exhibit the properties of a true tunnel barrier?

Here we discuss the results of a ballistic electron emission microscopy (BEEM) [5,6] and a scanning tunneling spectroscopy (STS) [7] study of the formation and electronic properties of ultrathin, thermally oxidized AlO<sub>x</sub> tunnel barriers. We monitor with nm resolution the formation of a tunnel barrier on an Al surface as the function of O<sub>2</sub> exposure, and observe the gradual reduction of the transparency of a Nb(or Co)-AlO<sub>x</sub>-Al-Nb(or Co) junction and the eventual development of a true energy barrier as the oxide layer forms and grows. This allows a direct determination of the AlO<sub>x</sub> barrier height and an examination of whether metallic pinholes or a distribution of single-electron channels through the oxide best describe its transport properties in the ultrathin limit.

Our samples were grown on H-passivated Si(111) substrates in ultrahigh-vacuum (UHV) both by thermal evaporation and by magnetron sputtering. The Si surface was first coated with a (111) normal oriented polycrystalline Au film to form a high-quality Schottky barrier for the BEEM measurements. The Au was then overcoated with a thin 1 nm Cu film which serves as a template for a transition

metal base electrode (either Co or Nb). The base electrode, typically 1.2 to 3.0 nm, was then deposited, followed by the Al film of thickness ranging from 0.6 to 1.5 nm. The Al layer was then exposed to O<sub>2</sub> for a fixed pressure and time, following which the top electrode (Co or Nb) was deposited and the sample studied *in situ* by BEEM. In some cases STS and BEEM measurements were made on the oxidized Al surface prior to the deposition of the top electrode.

In BEEM, a scanning tunneling microscope (STM) at a bias voltage  $V_t$  tunnel injects a current  $I_t$  into a conducting surface. These hot electrons then travel ballistically towards an underlying metal-semiconductor Schottky barrier interface. A fraction of the electrons that reach the interface and satisfy energy and any applicable momentum constraints can then pass into the semiconductor substrate, resulting in a BEEM collector current  $I_c$  that is detected by a separate BEEM amplifier. Those electrons that do not pass through the interface are collected by the STM amplifier. Thus  $I_c(V_t)$  provides a local measure of the energy-dependent ballistic transmissivity  $T$  of the conducting overlayer.

In the BEEM tunnel-barrier measurements,  $T$  of metal-AlO<sub>x</sub>-metal trilayers was examined as a function of the oxygen exposure the Al layer experienced prior to the deposition of the top electrode. In Fig. 1a, we show a typical  $I_c(V_t)$  result for a Co-Al-Co trilayer deposited on a Cu-Au-Si substrate without any exposure of the Al to oxygen, and one for the case where the Al has had a prolonged O<sub>2</sub> exposure. The first  $I_c(V_t)$  is essentially identical in form to that obtained with simple Au-Si Schottky barrier samples, and can be well fit with a free-electron BEEM model [8] that assumes strong scattering at the Schottky barrier interface, yielding a 0.82 eV barrier height. Figure 1b shows a series of BEEM  $I_c(V_t)$  measurements as obtained from different samples of essentially identical metal thicknesses, but with a progressively larger exposure of the Al layer to O<sub>2</sub>. In each case the results are typical of those obtained at various spots over a given sample; results which, with one exception discussed below, varied by less than 20% over the sample surface, including locations 10  $\mu\text{m}$  or more apart.

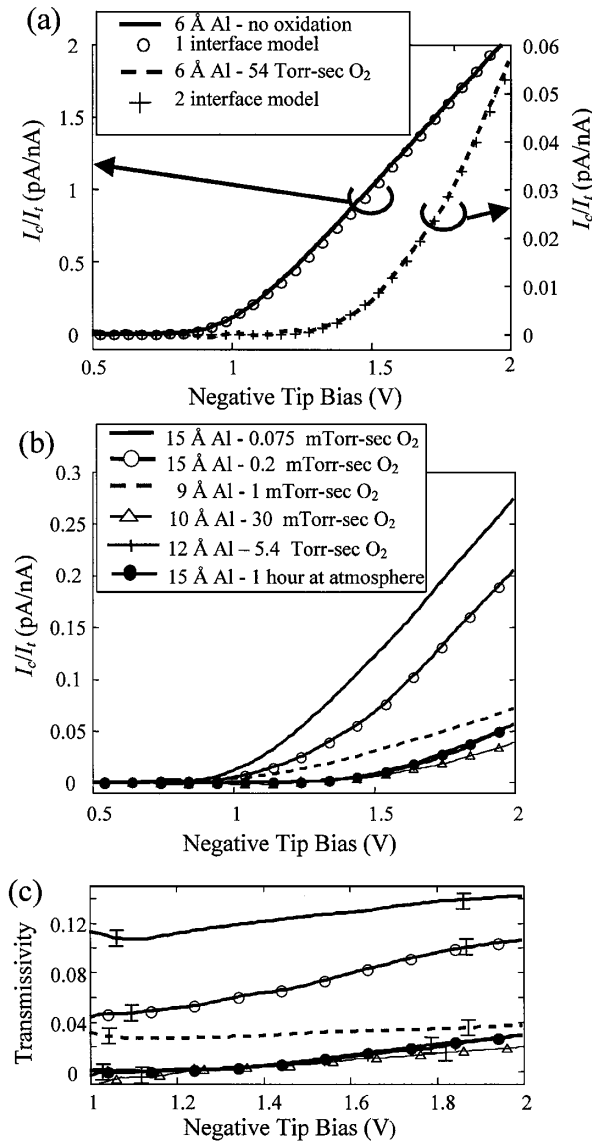


FIG. 1. (a) Normalized BEEM current vs STM bias,  $I_c$  vs  $V_t$ , for a Co-Al-Co trilayer film (solid line) and for a Co-AlO<sub>x</sub>-Al-Co thin film multilayer (dashed line) deposited on a Cu-Au-Si substrate. The open circles and crosses are fits to the data. (b)  $I_c$  vs  $V_t$  for a series of Co-Al-Co samples where the Al layer has received varying exposures to O<sub>2</sub> prior to the deposition of the top Co layer. (c) Junction transmissivity  $T$  obtained by normalizing the data in (b) by data from the unoxidized sample.

In Fig. 1c we plot the result obtained by dividing the  $I_c(V_t)$  data of the oxidized samples by  $I_c(V_t)$  of the unoxidized sample. This provides a measure of the energy-dependent  $T$  of the tunnel barrier as a function of oxygen exposure. The effect of the lowest exposure, 0.075 mTorr sec, is to attenuate  $T$  of the Co-Al-Co trilayer to about 0.1 at all bias levels above the 0.82 eV measurement threshold of the Au-Si Schottky barrier height. As the exposure is increased,  $T$  decreases further. Eventually, for doses  $\gg 1$  mTorrsec,  $T$  of the barrier at low bias, between 0.82 and 1.2 eV, is below our current measurement sensitivity,  $\sim 0.01$ , while beginning at 1.2 eV

the barrier transmissivity becomes observable and then increases with increasing bias. Once this behavior develops, increasing the oxygen exposure, which is known to form progressively higher impedance tunnel junctions [4], does not affect the high bias  $T$  of the barrier. Exposing the Al surface to air also does not alter  $T$ , nor does heating the exposed Al surface in air to 100 °C for 30 min prior to reintroducing the sample back into the UHV chamber and depositing the top electrode. We also note that Fig. 1 includes data from samples that have received much greater exposure to oxygen than has been shown, by analytical cross-section scanning transmission electron microscopy (STEM) [9], to be sufficient to fully oxidize a  $>1$  nm layer of Al.

We interpret these latter results as demonstrating that once the oxide layer becomes thick enough it develops an effective conduction band through which the ballistic electron beam can transit without appreciable “bulk” scattering. We find that the BEEM  $I_c(V_t)$  data for the strongly oxidized samples can be well fit by a generalized two-interface BEEM model. This assumes that, at both the Co-AlO<sub>x</sub> interface and the underlying Au-Si interface, the incident electron beam scatters isotropically, with the distribution of final states being dependent only on the relative density of states of the two materials at each interface [8]. This model makes a free electron assumption for the conduction bands of the oxide and metals and uses as fitting parameters the conduction band minimum of the oxide  $\phi_b$  relative to the Fermi level  $E_f$ , and the effective electron mass  $m_e$  of the oxide conduction band. The fit, shown in Fig. 1a, indicates that  $\phi_b = 1.2$  eV and  $m_e \approx 0.75m$ , where  $m$  is the free-electron mass.

While  $\phi_b$  is less than is often obtained by fits to TJ current-voltage ( $I$ - $V$ ) characteristics, this measurement does not involve any external bias being applied across the barrier, and it is not affected by the possible presence of low-energy electron channels that may provide low-voltage “leakage” through the barrier. With these values of  $\phi_b$  and  $m_e$  published, MTJ  $I$ - $V$ 's [10] can generally be well fit with Simmons' model [11]. While the band gap of sapphire is large,  $\sim 8.8$  eV [12], the structural disorder in amorphous aluminum oxide can result in very broad conduction and valence band tails [13]. A recent analytical STEM study of a AlO<sub>x</sub> tunnel barrier has shown a broadened conduction band edge that extends more than 4 eV below the band onset of sapphire [9].

The presence of a broad distribution of electronic states in the thin AlO<sub>x</sub> layers is confirmed by STS measurements. In Fig. 2a we show the normalized differential conductance  $d(\ln I_t)/d(\ln V_t)$ , which is approximately proportional to the density of electronic states at the surface of the sample [7], as obtained after exposure of the Al surface to three different oxygen dosages. We see that even after a prolonged O<sub>2</sub> exposure there remains a distribution of states that extends down to zero bias ( $E_f$ ) even though such dosages result in a tunnel barrier when the oxidized

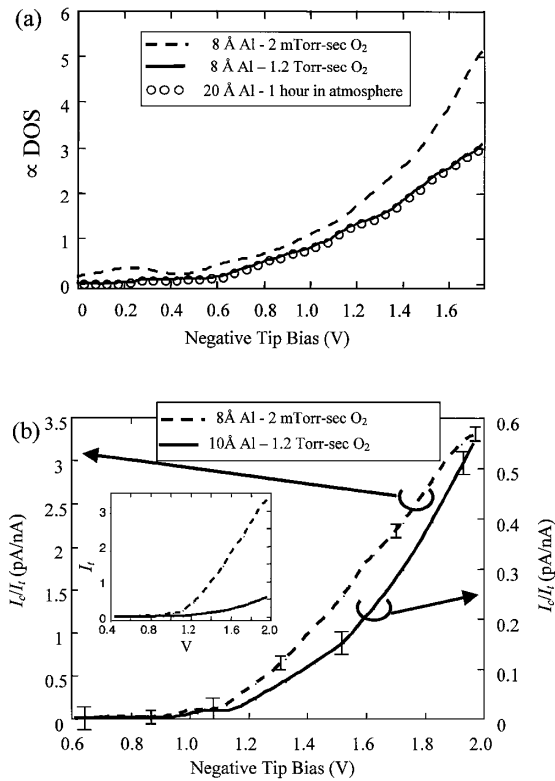


FIG. 2. (a) Normalized differential tunneling conductance  $d(\ln I_t)/d(\ln V_t)$  measurements, taken with an  $I_t$  set point of 0.25 nA at 2 V, made on the surface of Al after three different O<sub>2</sub> dosages; (b) BEEM measurements made on two oxidized Al surfaces without depositing a top electrode. The inset shows the un-normalized results.

surface is covered with Co (Fig. 1). BEEM measurements, shown in Fig. 2b, made in this case *before* the deposition of the top electrode sheds light on this apparent contradiction. There we see that, while there is a statistically significant BEEM current down to 0.9 V, there is a strong increase in  $I_c$  starting at about 1.1 V, both for the case of a 2 mTorr sec and a 1200 mTorr sec O<sub>2</sub> exposure. The BEEM measurement is predominately sensitive to those electrons that tunnel to *extended* states, and thus can directly travel ballistically to the underlying Schottky barrier interface, while the STS measurement examines both extended and localized states. Thus we conclude that after a sufficiently high O<sub>2</sub> exposure the latter dominate below 1.1 V. We interpret the  $\sim 0.1$  V difference in the oxide conduction band minimum indicated here from that obtained from the buried oxide BEEM measurements as arising from a small shift in the electrochemical potential of the oxide when the top electrode is deposited onto it.

Additional insight into the nature of the tunnel barrier can be obtained by considering previous JJ studies [4,14,15] in conjunction with this work. It has been shown that to produce Nb-AlO<sub>x</sub>-Al-Nb JJ's with  $J_c$  ranging from  $2 \times 10^5$  to  $1 \times 10^4$  A/cm<sup>2</sup> ( $R_n A$  ranging from 1 to 20  $\Omega \mu\text{m}^2$ ) requires an oxygen dose of  $\sim 400$  to 2400 mTorr sec [4]. To satisfactorily explain the superconducting  $I$ - $V$  charac-

teristics of such high-transparency junctions requires the presence of electron channels through the barrier at  $E_f$  whose individual transmission probability is  $\geq 0.5$ . Only with oxygen dosages such that  $J_c$  drops below  $10^4$  A/cm<sup>2</sup> (transparency  $\ll 10^{-4}$ ) does the density of these channels become negligible. The question is whether these channels are present as metal-filled "pinholes" [16], or are due to a small density of more or less uniformly distributed low-energy single-electron channels that extend through the thin disordered oxide layer. In the former case the rapid decrease in the density of conducting channels with increasing oxide thickness (oxygen dose) can be attributed to the resulting decrease in total pinhole area. In the latter case it can be attributed to the gradual transition to bulk oxide electronic properties as the lowest-energy oxide states become more and more localized, or move higher in energy.

BEEM measurements [6] have shown that if the Al layer is very thin,  $< 0.6$  nm for thermally deposited films and  $< 1.0$  nm for sputtered films, strong nanometer-scale inhomogeneities are generally found in both Co-AlO<sub>x</sub>-Co and Nb-AlO<sub>x</sub>-Nb junctions. But just slightly thicker Al layers, when oxidized, yield uniform barriers due to the excellent tendency of Al depositions to cover (wet) many transition metal surfaces. Thicker Al layers can be used for JJs, even for very high-transparency junctions, since because of the proximity effect not all the Al layer needs to be oxidized for good junction characteristics. (This incomplete Al oxidation approach is not suitable for MTJ applications.) In that case we find oxygen exposures  $> 30$  mTorr sec are sufficient to form apparently uniform barriers with no pinholes being detectable, even when scanning over areas  $\geq 1 \mu\text{m}^2$ . Only in the special situation when the oxygen dose is at the point,  $\sim 1$  mTorr sec, where a complete tunnel barrier just begins to form, can contrast variations in BEEM current intensity be seen, as illustrated in Fig. 3, but

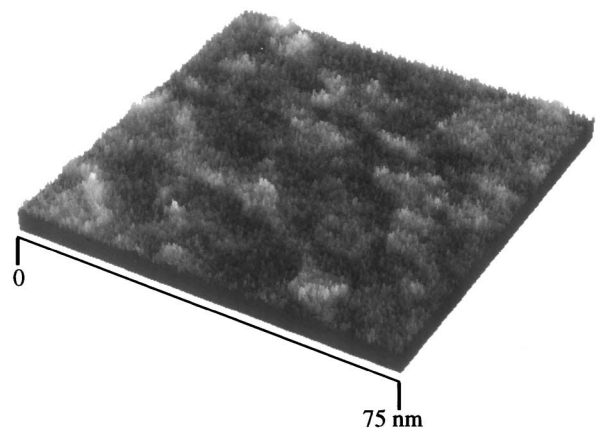


FIG. 3. A BEEM image ( $V_t = -1.5$  V) of a Co-AlO<sub>x</sub>-Al-Co sample where the Al surface was exposed to 1 mTorr sec of O<sub>2</sub>. The BEEM inhomogeneities are correlated with the individual grains in the film as determined from STM topography imaging. The gray scale ranges from 0 pA (darkest) to 0.5 pA (lightest). (The fine scale variations in the BEEM image arise from the noise limit of the measurement.)

this variation is on the scale of the individual grain size. This suggests the origin here is grain-to-grain variation in initial oxidation rates. At no point is  $I_c$  large enough to indicate the presence of a true metallic pinhole.

There has recently been strong interest in the electronic properties of ultrathin  $\text{SiO}_2$  thermally grown ( $>600^\circ\text{C}$ ) on Si, and in the issue of how thick the  $\text{SiO}_2$  layer has to be to obtain bulk electrical properties. Recent STEM electron energy loss studies have suggested that a 0.8 nm thickness is required [17]. A first-principles calculation [18] indicates that the local density of low-energy localized states in the oxide, and the magnitude of the energy gap, are explicitly related to the local environment of the oxygen atoms. This calculations indicates that bulk behavior develops only at an average distance of 0.5 nm from the Si- $\text{SiO}_2$  interface.

$\text{AlO}_x$  formed by near room-temperature oxidation, even if nearly stoichiometric  $\text{Al}_2\text{O}_3$  [9], is certainly more disordered than  $\text{SiO}_2$  grown by high temperature oxidation. The STS and STEM measurements show there is indeed a significant density of low-energy states in  $\text{AlO}_x$ , which we attribute to variations in the local atomic structure. The BEEM measurements indicate that when the oxide layer just begins to form, the hybridization of these oxide states with the electrodes provides direct conduction channels through the oxide resulting in a reduced interface transparency but one without substantial energy dependence. As the oxide layer grows, the decreasing overlap of the lowest-energy oxide states in the bulk of the oxide with those of the electrodes results in their gradual localization. The more disordered the oxide the more gradual and spatially variable this transition will be on the atomic scale. Until this localization is complete there will be single-electron channels distributed in the barrier, which can account for the subgap current of JJs. At higher energies,  $>1.2$  eV, the average density of states in the disordered oxide is sufficient that they form a band of extended states in the bulk whose lower edge,  $\sim 1.2$  eV, determines the oxide tunnel barrier height.

In summary, we find that the major issue in forming and understanding ultrathin  $\text{AlO}_x$  tunnel barriers is not pinholes with more than unit-cell dimensions, but is instead low-energy extended electron states in the very thin and disordered oxide, which only gradually become fully localized with increasing oxide thickness. To remove or reduce such states, which can affect the tunneling magnetoresistance behavior of a MTJ with low specific resistance as

well as the subgap-voltage conductance of a JJ with high  $J_c$ , will likely require a higher-temperature process [19] to form a more ordered oxide structure. This could result in a thinner transition to bulk insulating behavior, but the concomitant higher  $\phi_b$  [19] could be an undesirable tradeoff.

We thank Alan Kleinsasser and Monica Plisch for very helpful comments and suggestions. This research was supported by the Office of Naval Research and by DARPA. Additional support was provided by NSF through use of the facilities of the Cornell Center for Materials Research and the National Nanofabrication Users Network.

- 
- [1] M. Gurvitch, M. A. Washington, and H. A. Huggins, *Appl. Phys. Lett.* **42**, 472 (1983).
  - [2] J. S. Moodera, L. R. Kinder, T. M. Wong, and R. Meservey, *Phys. Rev. Lett.* **74**, 3273 (1995).
  - [3] D. Song, J. Nowak, and M. Covington, *J. Appl. Phys.* **87**, 5197 (2000).
  - [4] R. E. Miller, W.H. Maillison, A.W. Kleinsasser, K. A. Delin, and E.M. Macedo, *Appl. Phys. Lett.* **63**, 1423 (1993).
  - [5] W.J. Kaiser and L.D. Bell, *Phys. Rev. Lett.* **60**, 1406 (1988).
  - [6] W.H. Rippard, A.C. Perrella, and R.A. Buhrman, *Appl. Phys. Lett.* **78**, 1601 (2001).
  - [7] J. A. Stroscio and R. M. Feenstra, in *Scanning Tunneling Microscopy*, edited by J. A. Stroscio and W. J. Kaiser (Academic Press, San Diego, 1993), pp. 112–134.
  - [8] R. Ludeke and A. Bauer, *Phys. Rev. Lett.* **71**, 1760 (1993).
  - [9] M.J. Plisch, J.L. Chang, J. Silcox, and R.A. Buhrman, *Appl. Phys. Lett.* **79**, 391 (2001).
  - [10] For example, J.J. Sun, V. Soares, and P.P. Freitas, *Appl. Phys. Lett.* **74**, 448 (1999).
  - [11] J.G. Simmons, *J. Appl. Phys.* **34**, 1793 (1963).
  - [12] R.H. French, *J. Am. Ceram. Soc.* **73**, 477 (1990).
  - [13] I.A. Brytov and Y.N. Romashchenko, *Sov. Phys. Solid State* **20**, 384 (1978).
  - [14] A. W. Kleinsasser *et al.*, *Phys. Rev. Lett.* **72**, 1738 (1994).
  - [15] Y. Naveh *et al.*, *Phys. Rev. Lett.* **85**, 5404 (2000).
  - [16] See, e.g., B.J. Jonsson-Akerman *et al.*, *Appl. Phys. Lett.* **77**, 1870 (2000).
  - [17] D. A. Muller *et al.*, *Nature (London)* **399**, 758 (1999).
  - [18] J. B. Neaton, D. A. Muller, and N. W. Ashcroft, *Phys. Rev. Lett.* **85**, 1298 (2000).
  - [19] R. Ludeke, M. T. Cuberes, and E. Cartier, *Appl. Phys. Lett.* **76**, 2886 (2000).